AIAA 2004-0250

Bypass Transition on the Nozzle Wall of the Boeing/AFOSR Mach-6 Quiet Tunnel

Steven P. Schneider, Craig Skoch, Shann Rufer,
Erick Swanson, and Matthew Borg
Purdue University
West Lafayette, IN 47907-1282

This version corrects two minor errors from the printed version (Matt Borg's AIAA membership, and the year of the polish in item 4 on p. 18). It is the same as the uploaded version, except for the cover page.

42nd Aerospace Sciences Meeting & Exhibit
5–8 January 2004
Reno, Nevada

Bypass Transition on the Nozzle Wall of the Boeing/AFOSR Mach-6 Quiet Tunnel

Steven P. Schneider*, Craig Skoch†, Shann Rufer‡, Erick Swanson§, and Matthew Borg¶
School of Aeronautics and Astronautics
Purdue University
West Lafayette, IN 47907-1282

Abstract

Purdue University continues to develop a 9.5-inch Mach-6 Ludwieg tube for quiet-flow operation to high Reynolds number. Although the facility is operational, and stability measurements are underway, quiet flow has so far been achieved only at low Reynolds number. Bypass transition occurs on the nozzle wall, since the noise rises on the nozzle centerline at a total pressure of 8 psia, for all measured locations, beginning halfway down the nozzle. The bleed-slot flow was plumbed directly to the vacuum tank, eliminating jets that previously existing in the diffuser, but this had no effect on the onset of quiet flow. New measurements of the fluctuations in the diffuser also suggest that noise propagated from downstream is unlikely to be the cause of the bypass. Preliminary measurements of the nonuniformities and fluctuations in the contraction entrance leave open the question of whether these are sufficient to trip the nozzle-wall boundary layer. The wake of a probe in the contraction reduces the Reynolds number of quiet-flow onset but not dramatically. Preliminary measurements of condensation are also reported, along with preliminary hot-wire calibrations and hot-wire measurements of the fluctuations on sharp cones, and the successful fabrication of a new sting support.

*Associate Professor. Associate Fellow, AIAA.
†Research Assistant. Student Member, AIAA.
‡Research Assistant. Student Member, AIAA.
§Research Assistant. Student Member, AIAA.
¶Research Assistant. Student Member, AIAA.

Introduction

Hypersonic Laminar-Turbulent Transition

Laminar-turbulent transition in hypersonic boundary layers is important for prediction and control of heat transfer, skin friction, and other boundary layer properties. However, the mechanisms leading to transition are still poorly understood, even in low-noise environments. Applications hindered by this lack of understanding include reusable launch vehicles [1], high-speed interceptor missiles [2], hypersonic cruise vehicles [3], and reentry vehicles [4].

Many transition experiments have been carried out in conventional ground-testing facilities over the past 50 years. However, these experiments are contaminated by the high levels of noise that radiate from the turbulent boundary layers normally present on the wind tunnel walls [5]. These noise levels, typically 0.5-1% of the mean, are an order of magnitude larger than those observed in flight [6, 7]. These high noise levels can cause transition to occur an order of magnitude earlier than in flight [5, 7]. In addition, the mechanisms of transition operational in small-disturbance environments can be changed or bypassed altogether in high-noise environments; these changes in the mechanisms change the parametric trends in transition [6].

Development of Quiet-Flow Wind Tunnels

Only in the last two decades have low-noise supersonic wind tunnels been developed [5, 8]. This development has been difficult, since the test-section wall boundary-layers must be kept laminar in order to avoid high levels of eddy-Mach-wave acoustic radiation from the normally-present turbulent boundary layers. A Mach 3.5 tunnel was the first to be successfully developed at NASA Langley [9]. Langley then developed a Mach 6 quiet nozzle, which

was used as a starting point for the new Purdue nozzle [10]. Unfortunately, this nozzle was removed from service due to a space conflict. Langley also attempted to develop a Mach 8 quiet tunnel [8]; however, the high temperatures required to reach Mach 8 made this much more difficult, and the effort failed. The new Purdue Mach-6 quiet flow Ludwieg tube may become the only operational hypersonic quiet tunnel in the world, at least until the old Langley Mach-6 nozzle is brought back online.

Background of the Boeing/AFOSR Mach-6 Quiet Tunnel

A Mach-4 Ludwieg tube was developed at Purdue in 1992-1994 [11]. Quiet flow was achieved at low Reynolds numbers, and the facility was used for development of instrumentation and for measurements of instability waves under quiet-flow conditions. However, the low quiet Reynolds number and the small 4-inch test section imposed severe limitations.

A hypersonic facility that remains quiet to higher Reynolds numbers was needed. The low operating costs of the Mach-4 tunnel had to be maintained. Operation at Mach 6 was selected, since this is high enough for the hypersonic 2nd-mode instability to be dominant under cold-wall conditions, and high enough to observe hypersonic roughness-insensitivity effects, yet low enough that the required stagnation temperatures do not add dramatically to cost and difficulty of operation. Beginning with Ref. [12], a series of AIAA papers have reported on the design, fabrication, and shakedown, on the development of instrumentation, and on progress towards achieving quiet flow at high Reynolds number.

Ref. [13] summarized these earlier papers, and reported on initial quiet flow achieved at low Reynolds numbers with the 6th bleed-slot design, and also on initial measurements with temperature-sensitive paints and hot wires. Ref. [14] reported a detailed review of the literature for transition on blunt cones and the generic scramjet forebody, along with temperature-sensitive-paints results on the forebody, the results of the 7th bleed-slot throat geometry, and the results of polishing the downstream portion of the Mach-6 nozzle. Ref. [15] reported initial measurements of bypass transition on the nozzle wall, the elimination of low-pressure separation after removing the double-wedge model-support centerbody, and high levels of static-pressure fluctuations in the diffuser when the nozzle-wall boundary layer is laminar, as well as hot-wire and temperature-paints measurements on a sharp cone.

The present paper reports progress in the second half of 2003. The hot-wire measurements on the cone will be described first, followed by new efforts to increase the tunnel operating pressure to study transition on blunt cones at angle of attack. Measurements of the pitot and static pressures in the nozzle and diffuser will then be described, followed by measurements in the contraction entrance using a new hot-wire apparatus.

The Boeing/AFOSR Mach-6 Quiet Tunnel

Quiet facilities require low levels of noise in the inviscid flow entering the nozzle through the throat, and laminar boundary layers on the nozzle walls. These features make the noise level in quiet facilities an order of magnitude lower than in conventional facilities. To reach these low noise levels, conventional blow-down facilities must be extensively modified. Requirements include a 1 micron particle filter, a highly polished nozzle with bleed slots for the contraction-wall boundary layer, and a large settling chamber with screens and sintered-mesh plates for noise-reduction [5]. To reach these low noise levels in an affordable way, the Purdue facility has been designed as a Ludwieg tube [11]. A Ludwieg tube is a long pipe with a converging-diverging nozzle on the end, from which flow exits into the nozzle, test section, and second throat (Figure 1). A diaphragm is placed downstream of the test section. When the diaphragm bursts, an expansion wave travels upstream through the test section into the driver tube, and a fast valve is opened to initiate flow in the bleed slots. Since the flow remains quiet after the wave reflects from the contraction, sufficient vacuum can extend the useful runtime to many cycles of expansion-wave reflection, during which the pressure drops quasi-statically.

Figure 2 shows the nozzle. The region of useful quiet flow lies between the characteristics marking the onset of uniform flow, and the characteristics marking the upstream boundary of acoustic radiation from the onset of turbulence in the nozzle-wall boundary layer. The onset of turbulence is drawn for several computational predictions, although quiet flow has not yet been achieved except at very low Reynolds numbers. A 7.5-deg. sharp cone is also drawn on the figure. The rectangles are drawn on the nozzle at the location of window openings, all but one of which are presently filled with blank metal inserts. Images of the tunnel are available at `http://roger.ecn.purdue.edu/~aae519/BAM6QT-Mach-6-tunnel/`, along with ear-

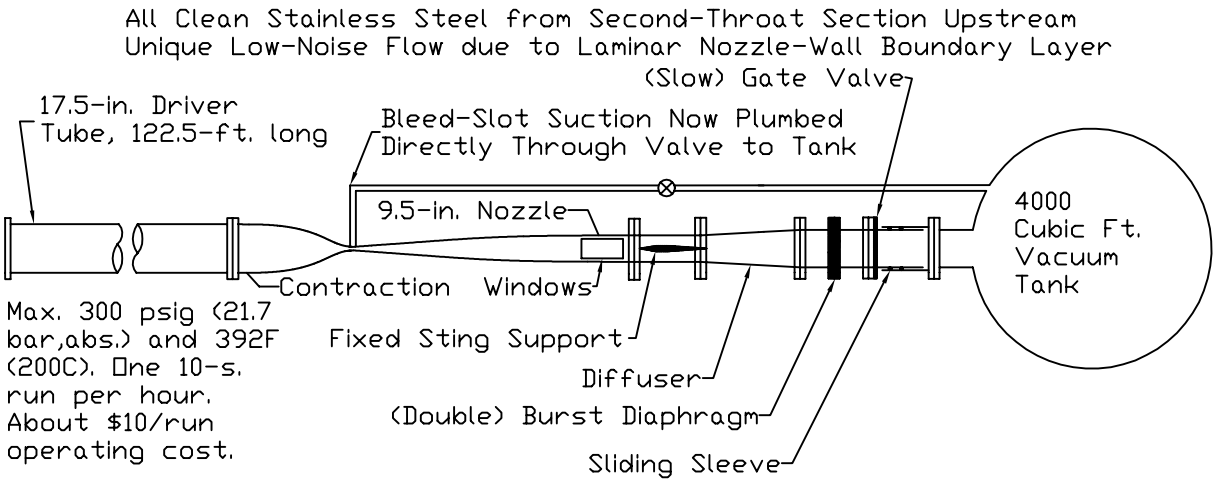

Figure 1: Schematic of Boeing/AFOSR Mach-6 Quiet Tunnel

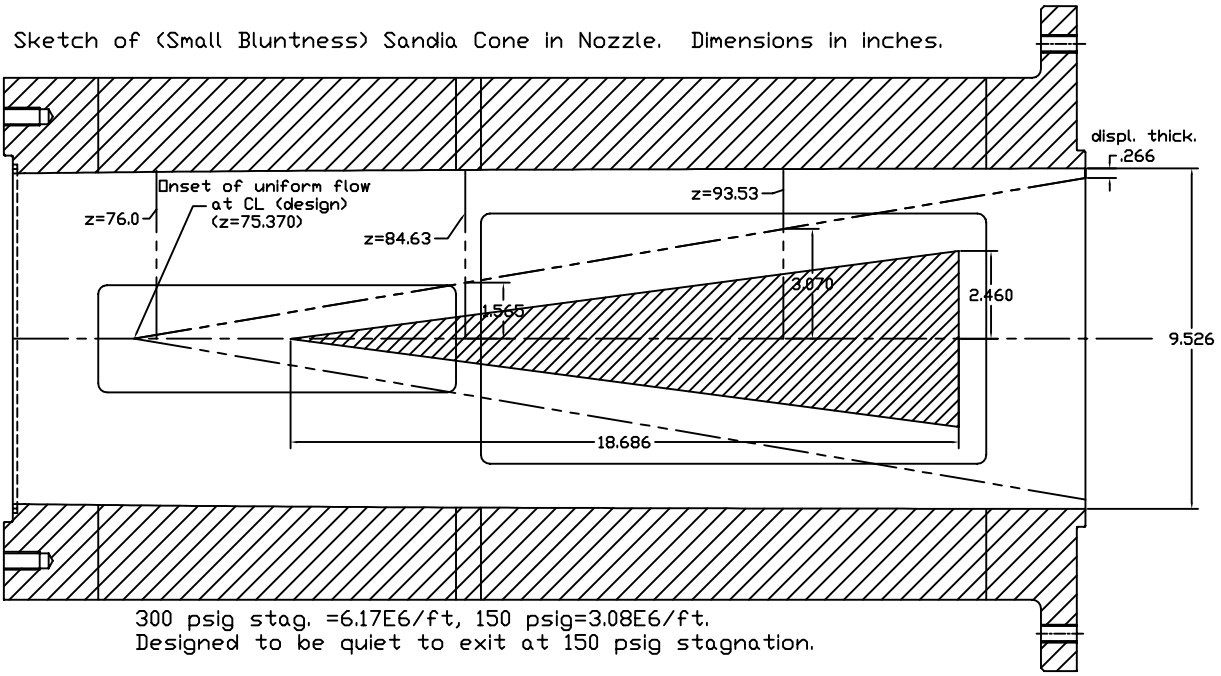

Figure 2: Schematic of Mach-6 Quiet Nozzle with Model

lier papers and other documentation.

Progress with the Hot Wire Measurements on Blunt Cones

Preliminary Hot-Wire Calibrations

The hot wires are calibrated in a small supersonic jet [16, 17]. The high levels of fluctuations mentioned in Ref. [18] were reduced by improvements in the settling chamber and contraction designs. A Mach 4 nozzle was designed and built for the calibrations, and a Mach 6 nozzle is to be built in the spring of 2004 to check the validity of Mach number independence above Mach 2. The supersonic jet allows for a continuous run with a 2.5 cm dia. nozzle at approximately Mach 3.8. The stagnation pressure and temperature in the jet can be varied independently, and measured using precision gauges and a J-type thermocouple.

In order to obtain accurate calibrations in the jet, cold wire, hot wire, and pitot-pressure measurements are needed. The hot wire can be placed in the center of the nozzle exit flow using a traverse. When connected to the low-current constant-current anemometer, the wire acts as a cold-wire temperature sensor and a profile of the stagnation temperature can be obtained. The wire is then connected to the TSI IFA-100 constant temperature anemometer (CTA), using the 1:1 bridge.

The hot wire used for the calibration procedure is made of Platinum/10% Rhodium (Pt/Rh), with a diameter of 0.00015 in., a length/diameter ratio of approximately 210, and a cold resistance of 10.5 ohms. The hot wire was placed in the center of the nozzle exit flow. The first set of runs was completed at a stagnation temperature of 290K, while varying the stagnation pressure from 10 to 90 psig. These measurements were then repeated. Later on the same day, a second pair of repeat measurements were obtained at 360K. Figure 3 shows the results. The plots of mean and RMS voltage show good repeatability. For the lower temperature runs, the two mean voltage curves are within 2% and for the higher temperature 1%. There is an offset of approximately 0.15 volts between the lower temperature runs and the higher temperature runs. The ratio of RMS to mean becomes large at low pressures, indicating a possible problem with flow quality in the calibration jet at low Reynolds numbers. Pitot measurements will be obtained to assess this problem.

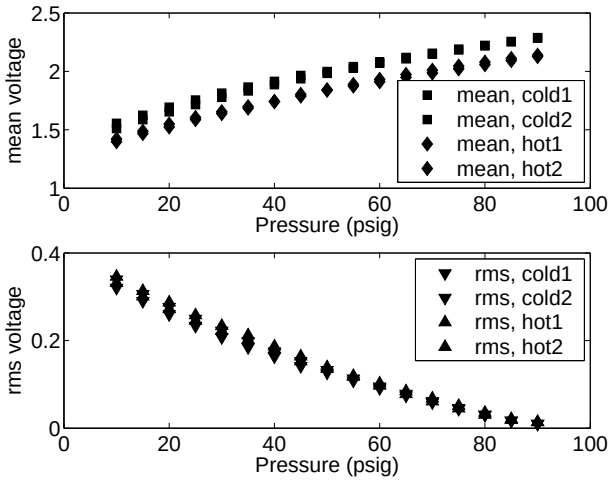

Figure 3: Hot Wire Calibrations Showing Repeatability

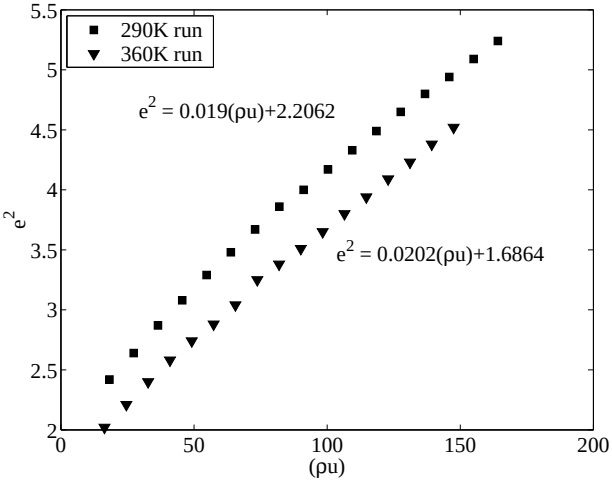

Figure 4: Hot Wire Calibrations for Massflux

A crude calibration was completed for the data obtained at both 290K and 360K. The Mach number in the center of the jet was earlier determined using measurements of pitot and stagnation pressure. The variation of Mach number with stagnation pressure was neglected here. This Mach number of 3.8 was then combined with the measured stagnation temperature and pressure and the assumption of isentropic flow to compute the mass flux in center of the jet. At each step, the pressure was increased by 5 psig, and the data were averaged over 25 seconds. The mass flow in $\mathrm{kg/m^2 - s}$ was then plotted against the square of the measured anemometer voltage to obtain the calibration curves shown in Fig. 4. Since the anemometer voltage from the jet was seen to be

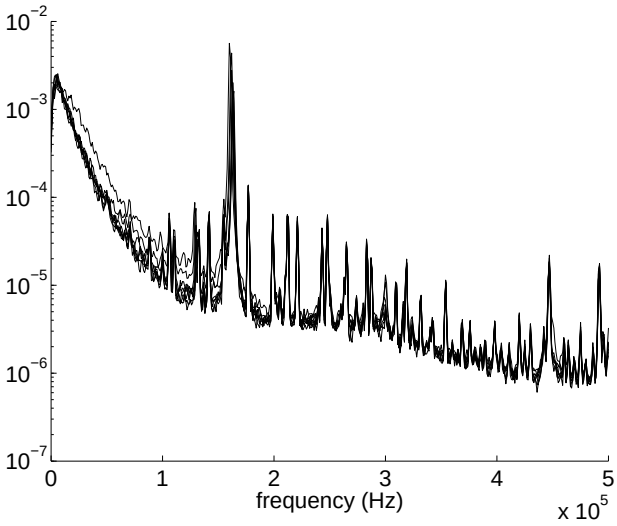

Figure 5: Hot Wire Spectra in Freestream

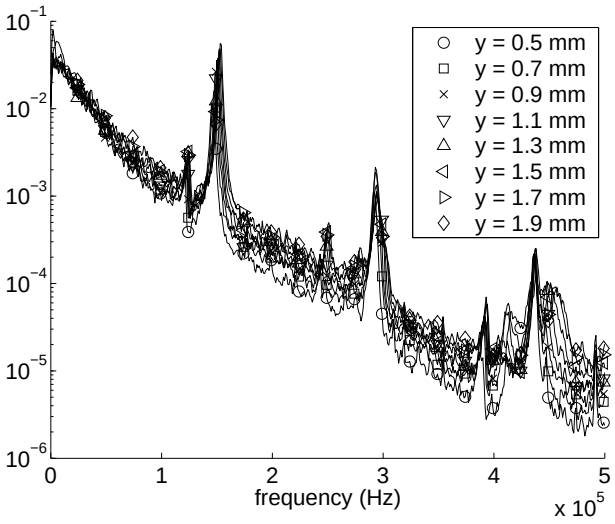

Figure 6: Hot-Wire Spectra in Boundary Layer on 5-deg. Cone

repeatable, one run was chosen for the calibration plot. The slopes of the curves are similar at both temperatures, within 5%.

Hot-Wire Measurements on Sharp Cones

Preliminary experiments were conducted in the Mach 6 tunnel on sharp cones with half-angles of 7 and 5 degrees. The hot wire used had a cold resistance of 9.8 ohms, an overheat of approximately 1.9 and a length/diameter ratio of 135. The frequency response was obtained from the square wave test, performed at atmospheric pressure in stagnant air before the run, as it is not practical to do a square wave test during the 4-8 sec. run. For the runs with the 7-degree cone the frequency response was 230 kHz, and for the 5 degree cone the response was 245 kHz. When testing with the 7 degree cone, the hot wire was placed approximately 16 inches back from the nosetip. For the longer 5-deg. cone, the wire was placed 21.5 inches from the nosetip (all distances are measured axially along the centerline). The 7-deg. cone is about 16.3 inches long, and the 5-deg. cone is about 23.5 inches long, so the measuring location is slightly upstream from the base.

The data was sampled using an 8-bit Tektronix TDS7104 digital oscilloscope in Hi-Res mode with a sampling frequency of 1 MHz. In Hi-Res mode, data is sampled at 1GHz and averaged on the fly into memory at the sampling rate. This provides additional resolution and digital filtering, both important for some of the data presented.

Fig. 5 shows the hot wire in the freestream of the tunnel with a driver pressure of 100 psia. All the measurements were made at a stagnation temperature of $160°C$. The dewpoint is uncertain. As can be seen here, there is a large spike in the spectra at about 160 kHz. This may be due to high-frequency oscillations in the hot-wire support.

Figures 6 and 7 were obtained from data taken during a 125 psia run with the 5 degree cone. Prior to the run, the hot wire was placed approximately 0.5mm from the cone wall. The wire is located here until 0.32 seconds after start-up and then is moved 0.2mm in 0.127 seconds. The wire then remains stationary for 0.1 seconds, and the process is repeated for 20 steps. For each 0.1-sec. record, power spectra are computed using a Hanning window in Matlab. The large spike seen here at 152 kHz may be related to the freestream spike at 160 kHz. The only major shift with probe location is better seen in the detail of Fig. 7. There is a bump in the spectra near 450kHz which is larger near the edge of the boundary layer, near 1.7 mm above the wall. It seems possible that this may be due to second-mode instability waves.

Figures 8 and 9 compare spectra for the 7 degree cone at 100 and 135 psia (at 1.3mm from the cone wall) with spectra from the 5 degree cone at 100 and 125 psia (at 1.7mm from the cone wall). The spectra for the two 5-deg. cone runs fall almost directly on top of each other. The main difference is that all the peaks for the higher pressure run are shifted to a slightly higher frequency. The spectra for the 7-deg. cone are slightly different. There is a much larger increase in amplitude and frequency of the

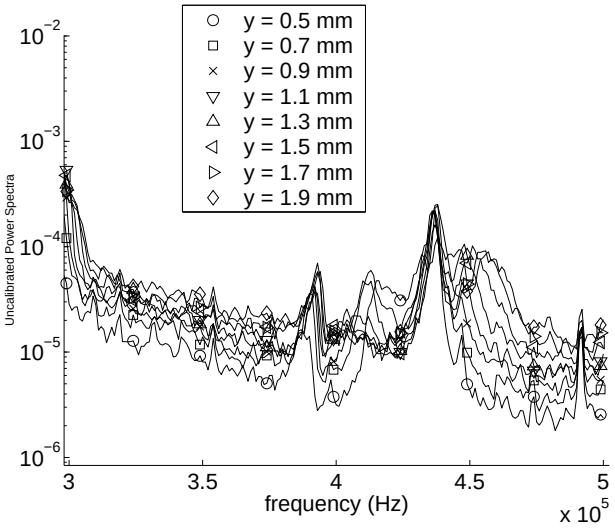

Figure 7: Detail of Hot-Wire Spectra in Boundary Layer on 5-Deg. Cone

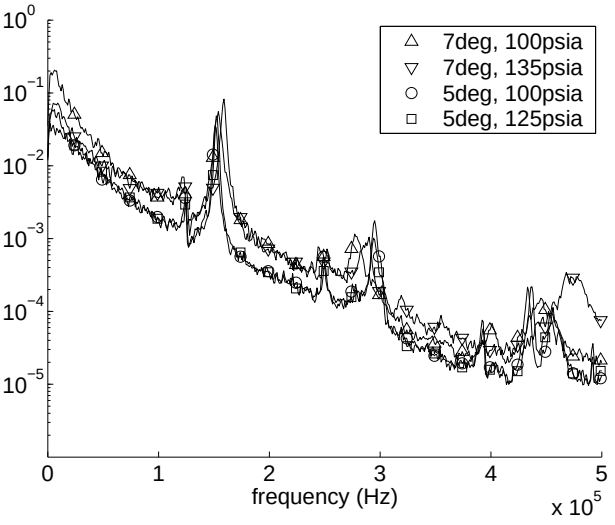

Figure 8: Hot-Wire Spectra in Boundary Layer on 5-deg. and 7-deg. Cone

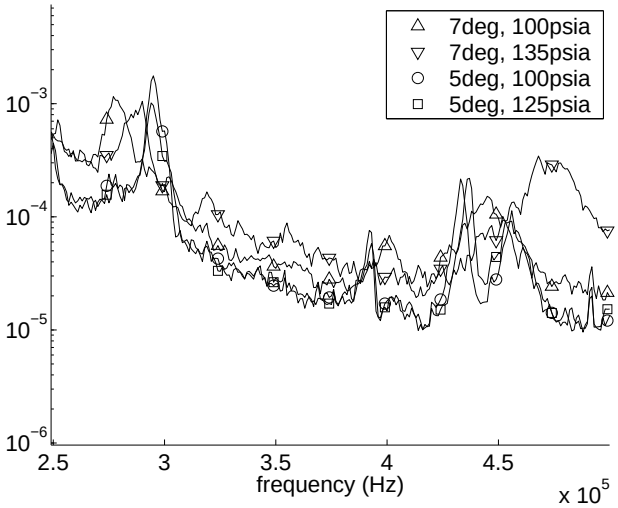

Figure 9: Detail of Spectra in Boundary Layer on 5-deg. and 7-deg. Cone

final peak in the spectrum, near 475 kHz. All of the spectra have a peak between 150 and 160KHz, which appears to be spurious.

These preliminary measurements suggest that instability waves might possibly be observed, but they are not yet clear. It was hoped that the longer 5-deg. cone would give a thicker boundary layer with lower frequency second-mode instabilities that are easier to observe, and the 450 kHz fluctuations in Fig. 7 might represent success. The data on the 7-deg. cone are also ambiguous. Work continues.

Towards High Reynolds Number Experiments at Mach 6

Motivation

Crossflow and roughness-induced transition are to be studied on blunt-nosed cones at angle of attack [19]. To obtain information on the transition mechanisms, affordable transition data is in many cases desirable. Measurements of this type are being undertaken in cooperation with Northrop-Grumman. The cones are to have 9-deg. half-angles and 3% bluntness, and are to be tested at zero and 9-deg. angles of attack, approximating proposed re-entry vehicles. Base radii will be 2.0 and 2.5 inches.

The necessary Reynolds number for these experiments was estimated by analyzing previous transition data taken at Mach 6 on cones of similar geometry [20, 21]. Both datasets were obtained at Mach 6 and in similar-sized tunnels, so transition in the

Purdue facility under conventional noise levels may be expected to occur at similar unit Reynolds numbers [6]. Ref. [20] suggests that at zero angle of attack, transition should occur on the cone beginning at a freestream Reynolds number of 8.5×10^6/ft for the 2-in. base radius model and at 6.7×10^6/ft for the 2.5-in. base radius model. Ref. [21] indicates that transition would occur on a cone with 2.5-in base radius and 1% bluntness at $Re_\infty = 3.6 \times 10^6$/ft and for a 4% blunt cone at $Re_\infty = 11.6 \times 10^6$/ft. The Reynolds number for a 3% blunt cone should be somewhere between these values.

Ref. [21] also presents tabulated data at angle of attack. For an 8% blunt cone, windward transition can be expected to occur on a 2.5-in. base radius cone at $Re_\infty = 13.6 \times 10^6$/ft, with leeward transition occurring at $Re_\infty = 2.7 \times 10^6$/ft. Thus, high Reynolds numbers are needed to study windward transition. For a 1% blunt cone, windward transition can be expected at $Re_\infty = 8 \times 10^6$/ft. The value for 3% bluntness will be in the range from 8×10^6 to 13.6×10^6/ft.

The Boeing/AFOSR Mach-6 Ludwieg Tube is rated for a maximum stagnation pressure of 300 psig, but is presently only operated up to about 130 psig. A boost pump has been added to enable us to reach the higher stagnation pressures, so that conditions for transition on blunt cones can be approached. The freestream Reynolds number was calculated assuming Mach-6 flow and using Keyes law to calculate viscosity [22]. Neglecting condensation, the maximum Reynolds number occurs at the maximum stagnation pressure and minimum stagnation temperature, 315 psia and 300K, and is 11×10^6/ft. Thus, the observation of windward transition may be possible if this high Reynolds number can be reached without difficulties with condensation (Refs. [23] and [24])

Condensation Tests

Condensation tests were undertaken to determine if it is feasible to drop the stagnation temperature in the Purdue Mach 6 Ludwieg Tube to increase the freestream unit Reynolds number above 6.4×10^6/ft, the Reynolds number obtained at a stagnation condition of 315 psia and 433 K. Tests were conducted at stagnation pressures of 37 psia through 134 psia and stagnation temperatures of 433 K, 413 K, 353 K, and 300 K.

The condensation tests were conducted by observing laser scattering from the condensed particles in the test section. A Uniphase He-Ne laser, operating at 20 mW with a wavelength of 633 nm, was directed into the test section through the window.

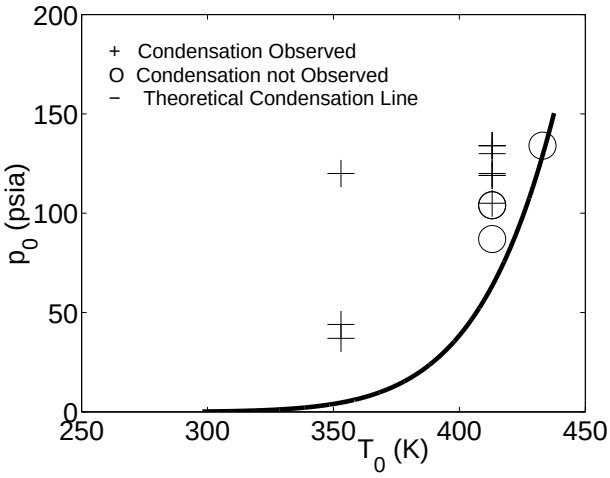

Figure 10: Observed Condensation and Calculated Saturation Pressures

The scattering was focused through a convex lens onto the sensor of a Hamamatsu H6780 photomultiplier tube. The sensor was covered with a red filter to allow only laser scattering to enter the PMT. The system was focused to the centerline of the test section by mounting a cardboard reflecter at the centerline and moving the lens until the laser reflection was focused on the filter in front of the PMT. The PMT output was recorded on a Tektronix TDS 7104 oscilloscope. The laser, lens, PMT, and optical mounts were provided by Prof. Steven Collicott of Purdue, who also provided valuable assistance in setting up and operating the apparatus.

Scattering was also observed visually. It was found during the course of the experiments that the PMT sensitivity was about the same as that of the eye, perhaps because of difficulties with the scattering of stray light in the PMT measurements. Scattering was most easily visualized by looking down into the test section through the top portion of the window, thus avoiding the scattering and reflections of the laser in the Plexiglas window. A piece of blue painter's tape was placed on the rear wall of the test section to cut down laser reflections.

The saturation pressure for the air in the tunnel was calculated for a given stagnation temperature using standard estimates of static liquefaction [23]. Static conditions were calculated through isentropic relations using a freestream Mach number of 6. The calculated saturation pressure line is compared to the observed condensation pressures in Figure 10. The plus signs indicate condensation was observed and the O's indicate that it was not. Some points overlap, as they were obtained at the same stagna-

tion pressure. The observation of both condensation and no condensation at 105 psia and 413 K is at present unexplained. The dewpoints for no condensation were $-16.7°C$ and $-11.3°C$, while for the condensing case the dewpoint was $-17°C$, thus no pattern with dewpoint is evident.

Condensation was not observed for a stagnation temperature of 433 K at dewpoints near $-6°C$. The observations at 413K and 353K were taken at dewpoints of $-6°C$ to $-21°C$ and $3°C$ to $-21°C$. Condensation was observed in earlier tests at 300 K, but the humidity was high at the low pressures where saturation is expected (this is because little dry air was pumped into the tunnel). High Reynolds number runs will most likely be made with drier air.

The results at 413K indicate that the observed condensation pressure is more than 50% larger than the calculated saturation pressure, since condensation was not observed at some pressures this high above the saturation line. Since these data were taken at lower dewpoints where less condensation is likely (the conditions at which high-Re tests will be run), a value of 50% was taken as representative of the potential increase in allowable stagnation pressure with supercooling. An estimate of the maximum unit Reynolds number can therefore be obtained using the 315 psia maximum pressure combined with the temperature required to avoid static liquefaction at 2/3 of 315 psia (210 psia and about 447K). This provides a maximum unit Reynolds number of about 6.7×10^6/ft, a minimal increase above the value at the static liquefaction limit. This maximum value indicates that we may be successful in obtaining transition at zero angle of attack on a 2.5-inch base-radius blunt cone near 3% bluntness, but at angle of attack transition on a smooth cone will be obtained only away from the windward ray.

Status of Quiet-Flow Performance

The primary focus of our work remains the achievement of quiet flow at high Reynolds number. During the second half of 2003, additional measurements were made well forward in the nozzle, to clarify the bypass transition and nozzle-wall boundary-layer separation that occur at low pressures. A new sting support was fabricated, to eliminate the separation while still allowing installation of models. A new path for the bleed air was also installed, to eliminate the jets that previously existing in the diffuser. Measurements were also made further aft in the diffuser and vacuum lines, to try to identify any noise sources that might propagate forward through the boundary layer and trip the upstream flow to turbulence. In addition, initial measurements were obtained in the contraction entrance with a new hot-wire apparatus, to begin to identify any noise sources that might be present in the flow leaving the driver tube.

Pitot Measurements Farther Forward With Double Wedge Model Support

To better understand the transition in the upstream portion of the nozzle, a 33-inch-long Pitot probe was earlier constructed to allow measurements farther forward in the nozzle [15]. The 3/4-inch diameter shaft is supported by a strut centered at $z = 76.421$ inches downstream of the throat. The shaft is tapered on the front, where an XCQ-062-15A Kulite pressure transducer is attached. Using this mount, Pitot measurements can be taken at $z = 45.03, 51.03, 57.03, 63.03$, and 69.03 inches, within 1/32 inch of the centerline. Measurements reported earlier with this apparatus showed that transition occured in the downstream half of the nozzle at essentially the same pressure [15]. Measurements made with the conventional pitot probe near the nozzle exit had earlier showed that a boundary-layer separation occurred in the aft end of the nozzle at low pressures when the double-wedge centerbody was installed [14, 15]. Additional measurements were needed to clarify these results.

Thus, six runs were made at $z = 45.03$ inches, for driver pressures of 8.04, 9.02, 10.03, 11.01, 11.02, and 14.31 psia. Three runs were made at $z = 57.03$ inches, for driver pressures of 8.03, 10.02, and 14.28 psia. Five runs were made at $z = 84.3$ in., for driver pressures of 7.98, 9.79, 9.98, 14.06, and 14.21 psia. The stagnation temperature was $160°C$ for all the runs.

Figure 11 shows the Mach number for various axial locations on the centerline. These measurements were made with the original double-wedge model support installed [25]. The driver tube pressure on the horizontal axis was measured near the contraction entrance and is averaged over 0.1 seconds. The Mach number is calculated using the Pitot pressure averaged over the same 0.1 seconds. The data were taken at 200 kHz with the Tektronix TDS7104 scope in High-Res mode. The separation that was noticed before at $z = 84.3$ inches can be seen here as a decrease in Mach number. At $z = 57.0$ and 45.0 inches, the large decrease in Mach number doesn't occur. This indicates that the separation does not extend this far forward. The farther forward measurements have a lower Mach number overall, but this is expected as the flow area is smaller

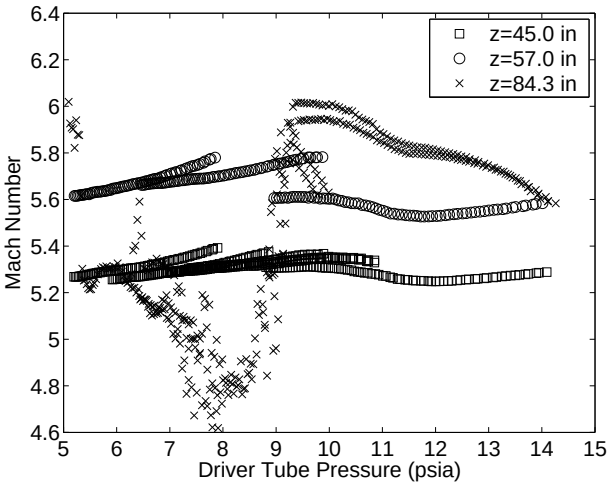

Figure 11: Axial Mach Number Distribution in Nozzle

at these axial locations [15].

Figure 12 shows the noise for the same runs shown in Fig. 11. The vertical axis in this plot shows the nondimensionalized RMS fluctuations, again averaged over 0.1 second segments. The noise drops to quiet levels at about the same pressure, at all axial locations in the downstream half of the nozzle. This suggests a bypass of the usual linear instability processes. The $z = 84.3$ data show a large increase in noise that corresponds to the large fluctuations that were seen just before the flow dropped quiet. This is not seen in the $z = 45.0$ and 57.0 inch cases. The noise drops quiet without the intermittent separation preceding it.

New Sting Support

Since the original sting support and second-throat insert caused separation in the nozzle-wall boundary layer at the low pressures where the flow became quiet, and since this separation disappeared when the insert was removed, a new sting support was needed to enable inserting models without the difficulty with separation. To enable vastly improved streamlining, the new design uses thin tensioned struts, following the suggestion of Dr. James Kendall, retired from JPL. The new support, shown in Fig. 13, uses a 2.5-in.-dia. cylinder with a 20-deg. chamfered leading edge to hold the 1.5-in.-dia. sting. The 1/8-in.-thick steel blades are welded to the center shaft and to 3/8-in.-square feet. The leading edge of the blades is tapered at 45 deg. The feet are chamfered at 20-deg. and torqued to pre-stress the blades to make the assembly rigid. A sting can be placed in the hole in the center of the shaft, with

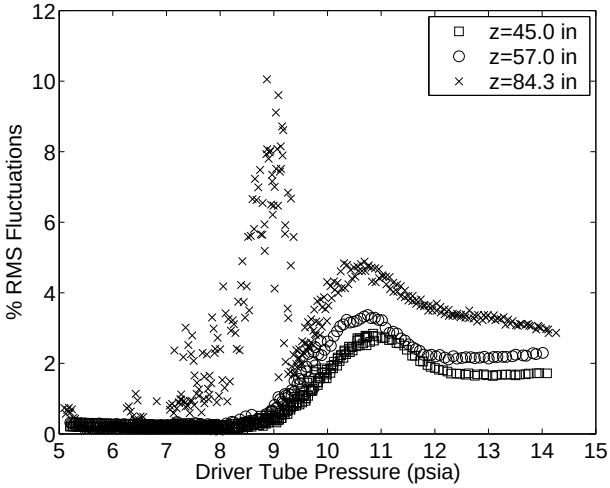

Figure 12: Axial Pitot-Fluctuation Distribution in Nozzle

Figure 13: Image of New Sting Support

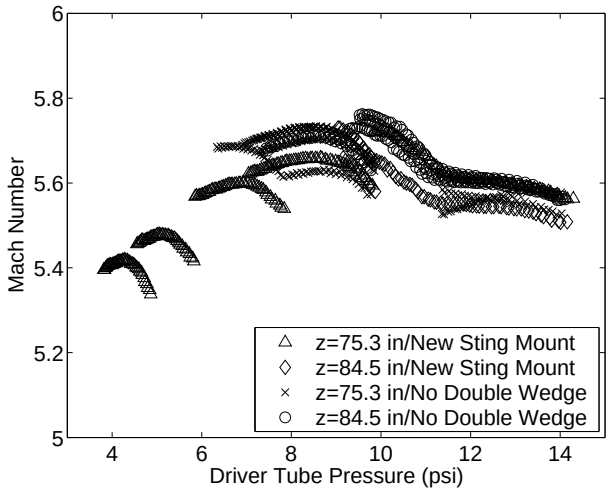

Figure 14: Mach Number with and without Sting Support

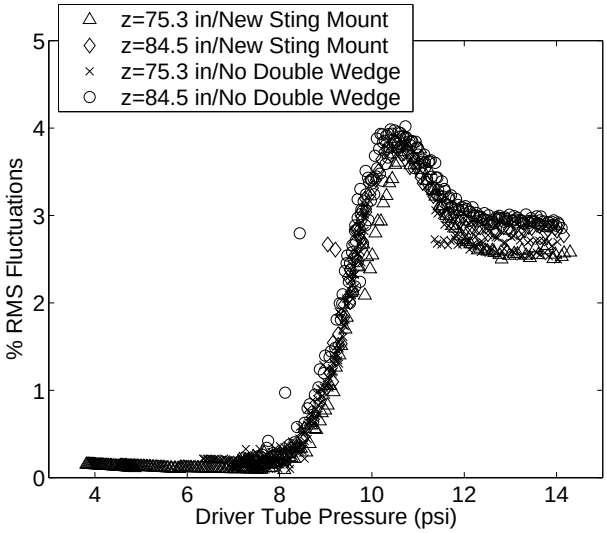

Figure 15: Pitot Fluctuations with and without Sting Support

set screws allowing adjustment of the axial location and also a fine adjustment of the angle of attack (following the design of the NASA Langley 20-inch Mach-6 tunnel per Scott Berry). The assembly was tested using a dummy sting. A torque of 623 ft.-lb. caused a deflection of only 0.0023 inches at a location 2.25 inches in front of the sting support.

Pitot measurements were made of the flow in the nozzle using the new sting mount. The tests in this section were performed with the hole in the center of the sting mount empty. Runs were performed at axial locations of $z = 75.3$ and 84.5 inches. Figure 14 shows the Mach number at these two locations for the cases with the old double wedge removed (empty tunnel) and with the new sting mount. All of these runs were performed with a driver tube temperature of $160°C$ and the Pitot probe on the centerline. The initial driver tube pressure was varied to get an idea of the behavior over a range of pressures. The Mach number seems comparable between the two cases, indicating that the new sting mount has eliminated the separation problem present with the old double wedge. This plot shows that the Mach number does drop at extremely low stagnation pressures near 4-6 psia, indicating extremely thick boundary layers or possibly separation, but these pressures are lower than are typically used in this tunnel.

Figure 15 shows the RMS pitot fluctuations for the same two cases. It shows that the noise drops out at the same pressure for all the cases. The stray points are apparently caused by large turbulent patches that occasionally dominate the 0.1-sec. averages. Since the noise drops out at the same driver tube pressure with both of these cases, and the large separations present with the double wedge are absent, this new sting mount should be successful in allowing a model to be placed in the tunnel without disrupting the tunnel flow.

New Bleed System

The bleed system that has been used for all of the runs previous to this section has been a passive system. This system, described in detail in Ref. [25], could possibly be responsible for large noise levels in the diffuser. These could feed forward through the subsonic part of the boundary layer, and possibly cause transition upstream. The original bleed system was passive, because the bleed flow was reintroduced to the tunnel upstream of the diaphragm section, so the bleed flow starts automatically when the tunnel was started. This was replaced with an active system that directed the bleed flow directly to the vacuum tank, eliminating the problem with reintroducing the bleed flow, but creating a problem with timing the start of the bleed flow.

To open the bleeds when the burst-diaphragms break to begin the main flow, this new system uses a fast-acting valve that is triggered when the run starts. A 3-in. dia. J.D. Gould solenoid valve is used, with a quoted opening time of 0.4-0.5 sec. and an operating pressure of 10 to 300 psi. A solid-state relay is used to control the valve. The 2-inch piping from the bleed slot to the valve is all clean stainless steel, to avoid problems with particulates that would travel from these lines past the throat during

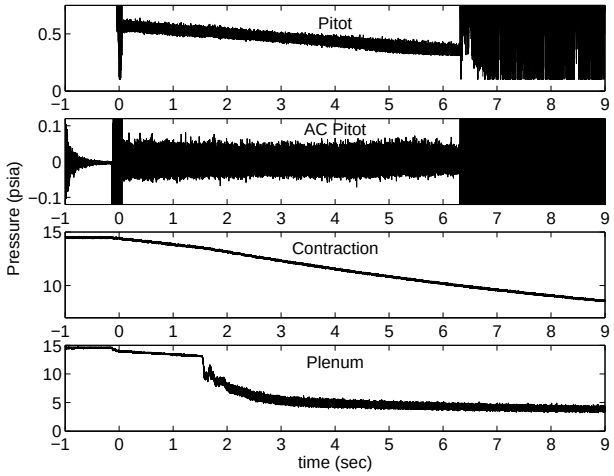

Figure 16: Typical Pressure Traces with New Bleed Lines

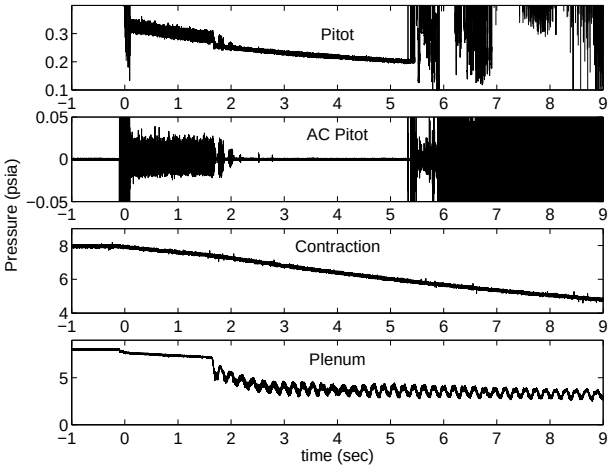

Figure 17: Pressure Traces at Lower Stagnation Pressure

the startup process, and possibly damage the highly polished finish. The line from the valve to the vacuum tank is 4-inch carbon steel.

Figure 16 shows pressure traces from the Pitot, contraction, and suction-plenum Kulites for a typical run with an initial driver tube pressure of 14.571 psia and a stagnation temperature of $160°C$. The pitot sensor was on the centerline at $z = 75.3$ inches. The plenum Kulite shows that at about 1.5 seconds after the flow started the valve has opened, and the air has been sucked out of the bleed lines. This is significantly longer than either the manufacturer-specified 0.5 sec. or the 0.25 seconds that was present with the original system [26]; however, it is acceptable for present purposes. The first part of the run is lost, and the run is shortened markedly, but there is no immediate evidence of noise being generated in the driver tube later in the run after the first wave reflection. The contraction trace shows a slight change in slope when the bleeds open, indicating that the massflow out of the driver tube increases, as expected. At this pressure, there appears to be little change in the pitot traces, as the flow is noisy with the bleeds open or closed.

Figure 17 shows the same traces for a run with an initial driver tube pressure of 7.977 psia. The pitot sensor is located at $z = 75.3$ inches and the stagnation temperature is again $160°C$. The plenum pressure seems to drop at about the same time into the run, but there is an oscillation present after this. This is because the bleed valve requires a pressure difference across it to hold it open. At the low pressures used here, there is barely enough pressure difference, and the valve flaps. The Pitot

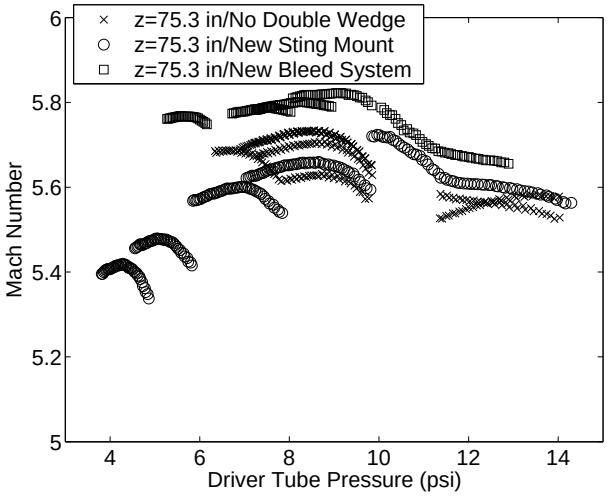

Figure 18: Mach Number for New Configurations

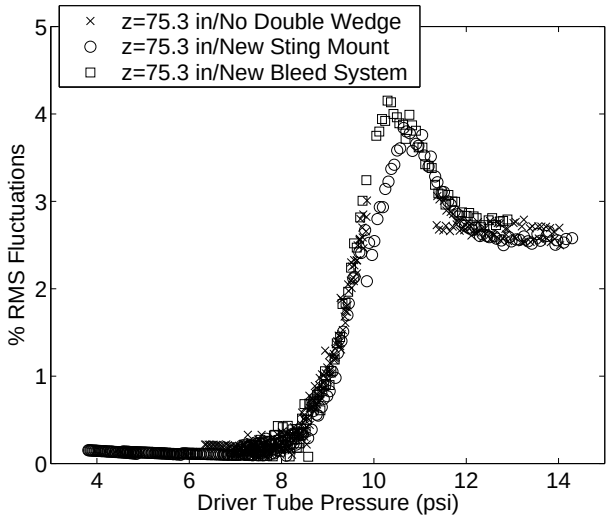

Figure 19: Pitot Fluctuations for New Configurations

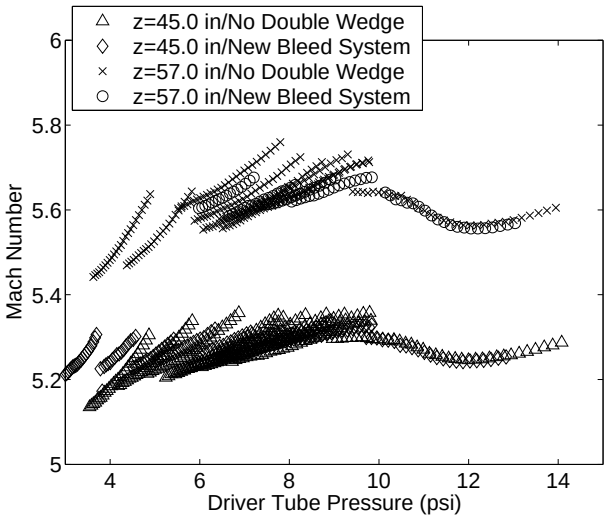

Figure 20: Mach Number Forward in Nozzle for New Configurations

traces show noisy flow at the beginning of the run, when the bleeds are not yet open, and this drops quiet after the pressure in the suction plenum has dropped low enough to allow choked flow through the bleed slot. The Pitot trace seems to have intermittent quiet flow near the beginning of the active bleed slot flow, probably due to the plenum pressure oscillating above and below the pressure necessary for choked flow. It should be noted that once there is choked flow through the bleed slot, the fluctuations in the suction plenum do not appear to feed forward and affect the main flow.

Figure 18 shows the Mach number at $z = 75.3$ inches for the configurations with no double wedge, the new sting mount, and the new bleed system for varying driver tube pressures. These runs were again obtained at a stagnation temperature of $160°C$. Since the runs were all made below atmospheric pressure, dewpoint measurements were not available. The runs without the double wedge were performed for initial driver pressures of 8.01, 10.01, 10.07, 10.08, 10.09, and 14.36 psia. The runs with the new sting were performed at driver pressures of 5.02, 6.01, 8.01, 10.01, and 14.41 psia. The runs with the new bleed system were performed at 6.83, 8.91, 10.00, 10.96, and 14.42 psia; these also use the new sting mount.

Fig. 18 shows that the Mach number is slightly higher with the new bleed system, though the change is not extremely large. This higher Mach number is surprising, and may possibly be caused by the difference in the noise feeding forward from the diffuser within the boundary layer. Figure 19 shows the noise for the same cases. This shows that the noise for all of the cases drop out at about the same driver tube pressure, although the noise rises slightly higher with the new bleed system case before dropping. Disappointingly, this shows no effect on quiet flow of the noise generated by the bleed-slot-air jets in the diffuser.

Figure 20 shows the comparison between the configuration with no double wedge and with the new bleed system, for locations farther forward in the nozzle. Again, the runs with the new bleed system use the new sting mount. This plot shows little difference between the Mach numbers in the two cases. Figure 21 has the comparison for the RMS noise values. The noise for both configurations and both locations drop out at about the same driver tube pressure. At $z = 57.0$ inches, the noise using the new bleed system rises higher than for the no-double-wedge case before it drops out.

In summary, the new sting support performs well, as it does not seem to affect the flow, as compared to an empty tunnel. However, the new bleed-slot plumbing that avoids the diffuser-section jets is a disappointment, since it seems to have no effect on the onset of quiet flow. Since a number of different effects can combine to cause transition, it is not certain that the bleed jets did not affect transition, but the lack of an effect when they are removed suggests that another cause for the early transition should be sought.

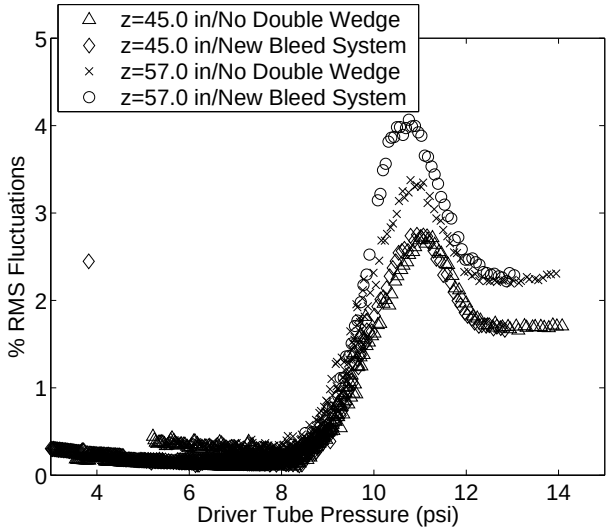

Figure 21: Pitot Fluctuations Forward for New Configurations

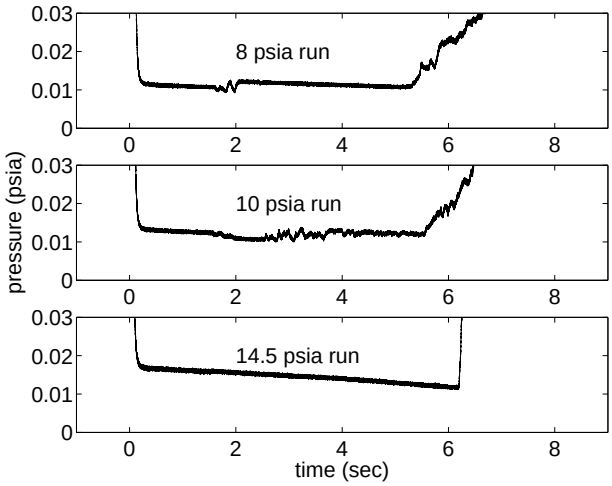

Figure 23: Static Pressure Traces in Nozzle at $z = 75.7$ in.

Diffuser Measurements

Additional 1/4-20 holes were drilled and tapped at various locations in the diffuser and vacuum lines. These allow installing flush-surface XCQ-062-15A Kulites to observe what is happening farther downstream of the test section. Fig. 22 shows the diffuser traces for various z-locations, for an initial driver pressure of 7.97 (±0.10%) psia; similar data were also obtained at 10.00 (±0.10%), and 14.56 (±0.15%) psia. The initial vacuum tank pressure was 2.0 torr and the driver tube temperature was $160°C$. The Kulite at $z = 75.7$ inches is in the nozzle, the one at $z = 105.0$ inches is just in front of the new sting mount, and the ones at or beyond $z = 263.0$ inches are after the diaphragm section. The pressure measurements are not very accurate, since the accuracy of the Kulites is only about 0.015 psia. For Mach 6 flow and a driver tube pressure of 14.5 psia, the expected static pressure is 0.009 psia. Because of the lack of accuracy in these measurements, no Mach number data is calculated based on the diffuser measurements. These measurements were carried out with the new bleed system, a pitot probe installed in the nozzle, and the new sting support system present, but empty, without a model.

The traces generally show pressure rises beginning in the aft sections of the vacuum piping, and moving forward as the pressure in the vacuum tank rises during the run. At the two stations aft of $z = 400$ inches, the pressure rises smoothly. For the four stations between 180 and 310 inches, a sharp rise is seen near 2-3/4 sec., possibly indicating a shock wave propagating forward. Some of the traces show high levels of fluctuations, and some show low levels. It is not yet clear whether the fluctuations are a natural feature of the flow, or are connected to the limited accuracy with which the transducers can be mounted flush with the wall.

Figure 23 shows a detail of similar static pressure data for three different pressures at $z = 75.7$ in. Pitot traces, not shown here, reveal that the 8 psia run is entirely quiet after the bleeds open, the 10 psia run is transitioning to quiet, and the 14.5 psia run is noisy throughout the run. The noise that can be seen in the 8 psia and 10 psia traces at about 1.5 to 2 seconds into the run occurs when the bleeds open. Figure 24 shows the same data for $z = 104.85$ in. This shows a similar higher noise for the 10 psia run when the tunnel is transitioning to quiet flow. Figure 25 shows the same data at $z = 206.25$ in. This data rises earlier since it is farther back in the diffuser, but a rise in noise can still be seen in the 10 psia run before this occurs.

Figure 12 in Ref. [15] showed the effect of throttling the bleed valves with the original double wedge present. That data was at $z = 104.85$ in. using an initial driver tube pressure of 10 psia. This plot showed a high level of noise when the bleeds were operating. This noise appears to still be present with the new sting mount, but only for the 10 psia runs where the tunnel is transitioning between noisy and quiet flow. When the tunnel is either completely noisy or completely quiet these large fluctuations do not appear. There is little evidence of large fluctuations propagating forward from the diffuser into

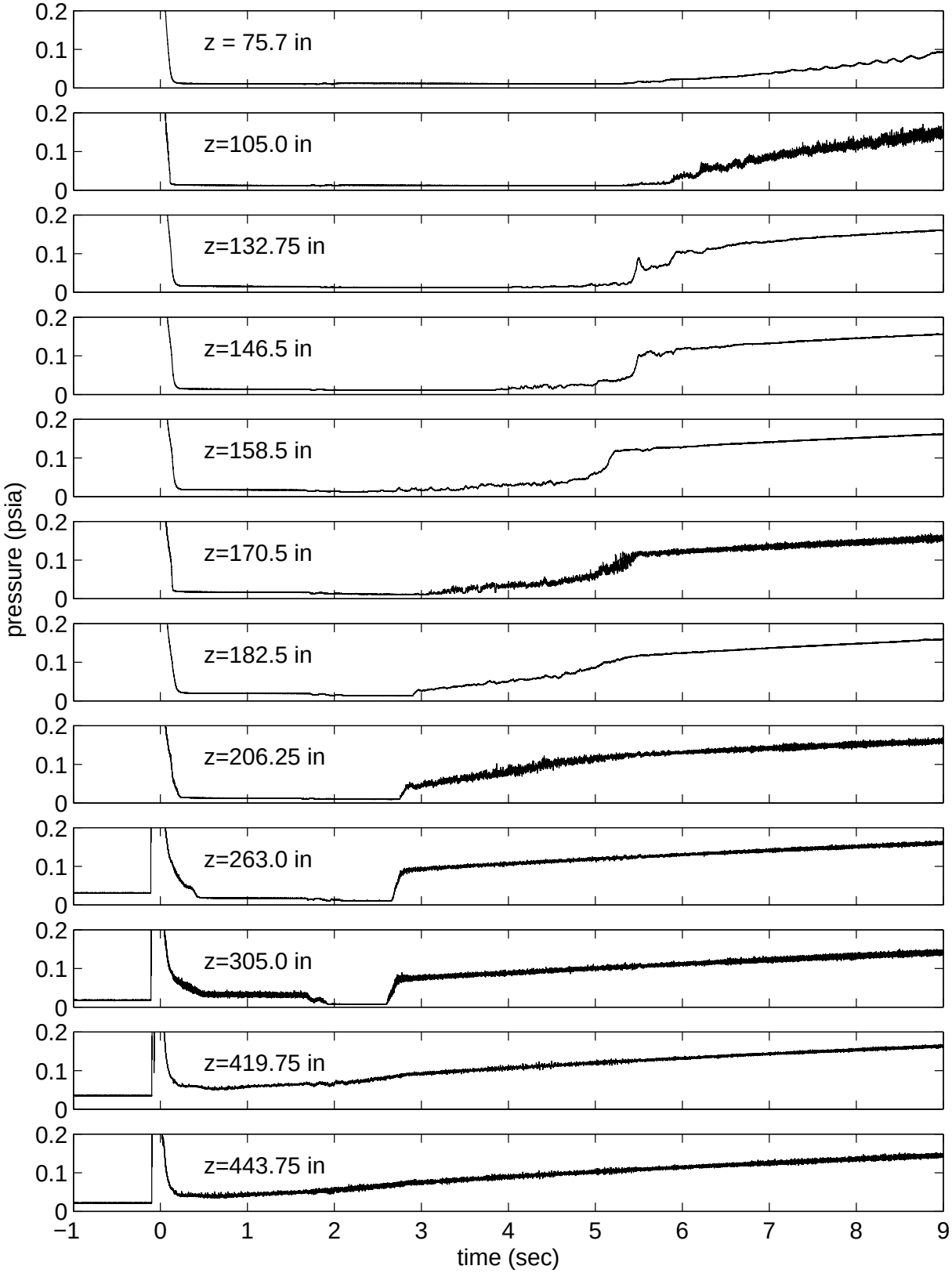

Figure 22: Static Pressure Fluctuations in Nozzle, Diffuser, and Vacuum Lines at 8 psia

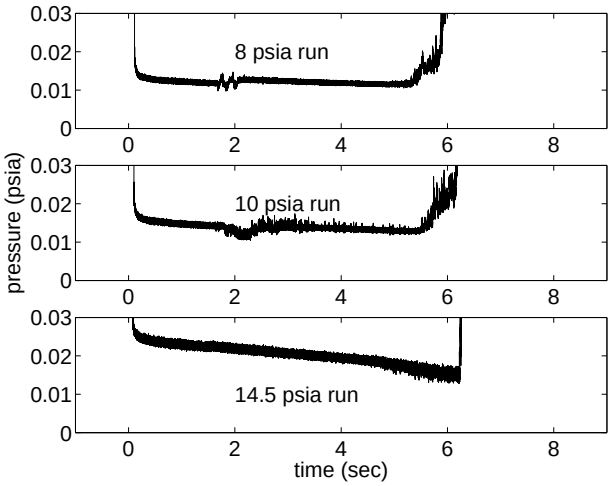

Figure 24: Static Pressure Traces in Diffuser at $z = 104.85$ in.

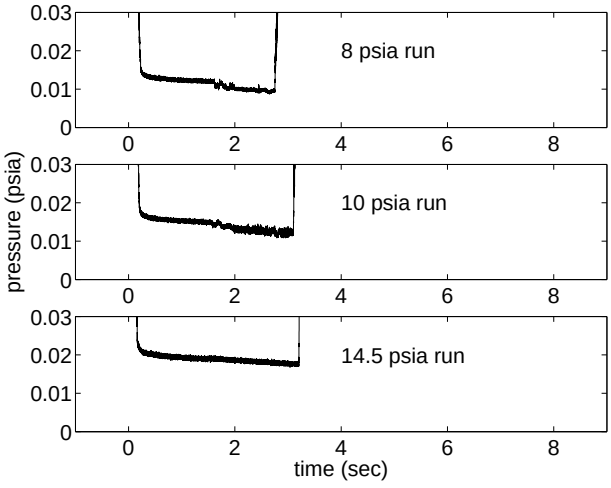

Figure 25: Static Pressure Traces in Diffuser at $z = 206.25$ in.

the nozzle, suggesting that the problem with early transition on the nozzle walls is probably not due to disturbances generated in the diffuser downstream.

Preliminary Measurements in Contraction Entrance

Measurements in the contraction entrance are also needed, to assess any disturbances that may be exiting the driver tube and causing early transition in the nozzle-wall boundary layer. The Mach number in the driver tube is about 0.003 [27], so the velocity in the contraction entrance is very low. Preliminary hot wire measurements were made in the contraction using the Tektronix scope at 200 kS/s in high resolution mode. The wire was a TSI Model 1222-P12.5 high-temperature platinum-iridium probe, with a 6.3-micron dia. and a 1.27-mm length. The cold resistance was 11.37 ohms, while the overheat ratio and square-wave frequency response for the first run were 1.35 and 73.0 kHz respectively. For the other runs, the overheat ratio was approximately 1.45 and the frequency response was approximately 70.1 kHz. The driver tube was heated to $85°C$, while the air entering the driver tube was heated to $105°C$, and the contraction was not heated. The inconsistency between $85°C$ and $105°C$ was an oversight. These temperatures were lower than normally used, to ease operations with the port at the contraction entrance; difficulties with the temperature of the driver air are to be addressed later.

A hot wire probe was inserted into the contraction via the 1-inch instrument port at $z = -34.47$ inches, upstream of the throat. At this location, 6.500 inches downstream of the beginning of the contraction section, the tunnel radius has decreased only slightly, from 8.750 inches to 8.705 inches, so the conditions are a close approximation to those at the end of the driver tube. The center of the insert with the contraction-entrance static-pressure tap is located at the same streamwise location. The probe was connected to a TSI IFA-100 constant temperature anemometer (CTA). The standard bridge was used, and these initial results are uncalibrated. All of these initial runs were made at a stagnation pressure of 100 psia.

Hot wire measurements were made with the probe at approximately $y = 1.56$ in., 2.56 in., 3.56 in., 4.56 in., 5.56 in., and 6.84 in. down from the top tunnel wall. Measurements were made once at each location, but will later be checked for repeatability. Figs. 26 and 27 show sample traces with the probe located 3.56 and 2.56 inches below the wall.

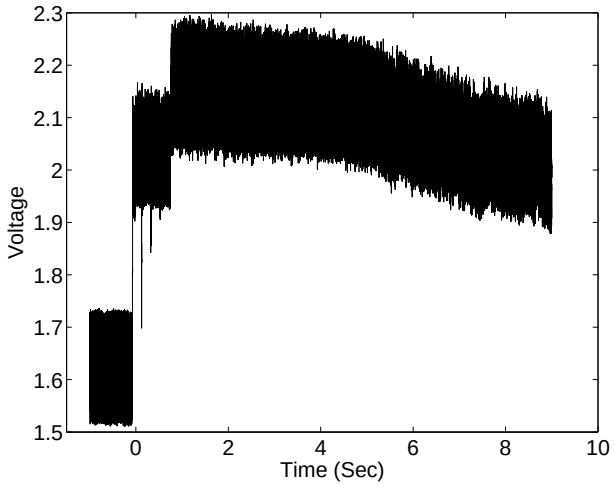

Figure 26: Sample Hot-Wire Fluctuations in Contraction Entrance at $y = -3.56$ inches

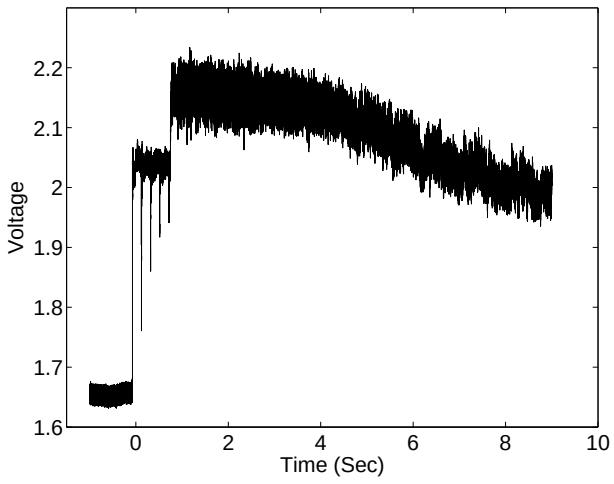

Figure 27: Sample Hot-Wire Fluctuations in Contraction Entrance at $y = -2.56$ inches

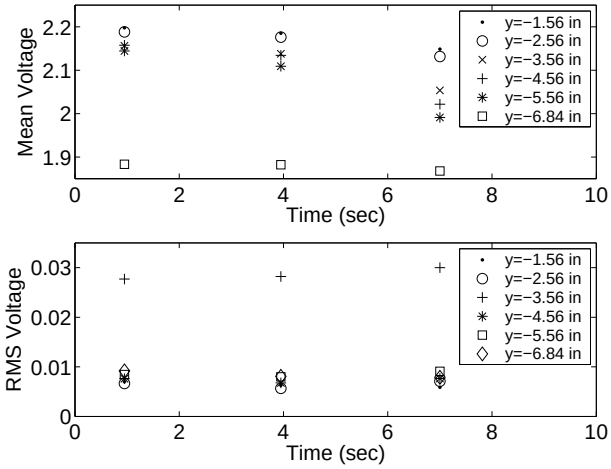

Figure 28: Hot-Wire Fluctuations in Contraction Entrance

The data prior to 0 seconds represents the pre-run data. The initial sharp rise coincides with the start of the run. The second sharp rise at approximately 1 second is due to the massflux increase caused by the opening of the bleed valve. The fluctuations at intervals of approximately 200 ms are probably due to the expansion waves passing the hot wire during the run. Hypersonic flow in the nozzle ended at approximately six and one half seconds.

The first plot in Fig. 28 shows the mean voltage from the CTA for three time periods of 0.2 seconds each. The time periods were chosen to correspond to a pressure drop due to expansion waves passing through the contraction. The time periods straddle the period of a pressure drop. There is a discrepancy in the mean data at y=-6.84 in. This is possibly due to lower scope resolution during the first run; no repeatability data exists yet. The second plot of Fig. 28 is the RMS voltage over the aforementioned time periods. There is an obvious discrepancy in the data for y=-3.56 inches which is as yet unaccounted for. The trace for this run can be seen in Fig. 26. When compared to Fig. 27, it can be seen that the signal from the hot wire was much noisier in the former run. This could be due to some external source of noise, although this run was made within 2 hours of previous run.

The mean voltage drops monotonically with distance from the upper tunnel wall, suggesting a nonuniform core flow, which would be a concern. The fluctuations at all vertical tunnel locations tested were about two orders of magnitude lower than the mean, which suggests they are reasonably low. It was desired to compare the pre-run noise to

that during the run to better understand the fluctuations. The RMS was calculated for the 0.2 seconds around the center of the pre-run time. With the exception of the data for $y = -6.84$ in. and $y = -3.56$ in., the pre-run noise was about an order of magnitude less than the noise during the run. Thus, the fluctuations in the driver tube increased significantly from the pre-run to the actual run for most y locations. This raises some concern about the level of these fluctuations.

The pre-run noise for $y = -6.84$ in. was 14.1% higher than the RMS calculated at the first time station during the run. This could be because for this run there was less pre-run time than for all other runs. The lower scope resolution for this run probably also contributed to these results. The pre-run noise for $y = -3.56$ in. was 34.4% lower than the RMS calculated at the first time station during the run. This discrepancy is probably due to some external source of noise since the resolution on the scope was set sufficiently high and there is not much observable difference between pre-run noise and that during the run.

In summary, preliminary uncalibrated hot-wire measurements showed that the velocity fluctuations in the contraction section were around two orders of magnitude less than the mean, suggesting a low noise level. However, the pre-run fluctuations were generally around an order of magnitude lower than fluctuations calculated at the first time station during the run, raising a concern about the measurable level of noise. In addition, the apparent nonuniformity of the mean flow raises additional concerns. Calibrated measurements are to be carried out in multiple repeated runs so that this source of disturbances can be better evaluated.

Preliminary Measurements in Nozzle as Affected by Contraction

It was desired to observe whether the presence of a hot wire probe inserted in the 1 inch instrument port of the contraction section approximately 7 inches down from the upper tunnel wall would upset the fully quiet flow observed near the nozzle exit at a driver tube pressure of 8 psia. For these measurements, the pitot sensor was placed on the tunnel centerline at $z = 84.3$ inches.

Fig. 29 shows the nozzle-exit pitot measurements with and without the hot wire probe in the contraction section. The first plot shows the quiet flow without the probe; the second plot shows the flow with the hot wire probe in the stream. The probe initially upset quiet flow, but quiet flow did eventually resume after the driver tube pressure had dropped enough.

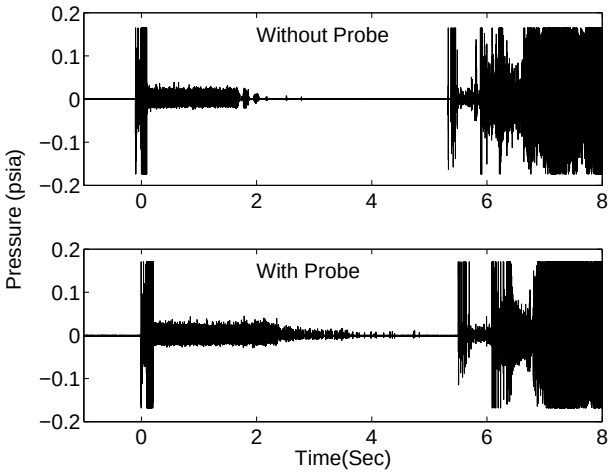

Figure 29: Pitot Fluctuations in Nozzle with and without Obstruction in Contraction Entrance

It is also desired to ascertain whether the temperature profile in the nozzle is constant, in order to see if any tunnel noise can be attributed to convection currents set up by a temperature gradient. A simple way to address this issue was to obtain cold-wire measurements in the nozzle, approximately 87 in. downstream of the throat. The wire was Platinum/10% Rhodium (Pt/Rh), had a cold resistance of 9.9 ohms, a diameter of 0.00015 in. and an L/d of 135. In order to measure the temperature profile, the hot wire was connected to a constant current anemometer (CCA). Measurements were made at centerline, one inch above and below the centerline, 1.8 inches above and below the centerline, and 2.72 inches above the centerline. Fig. 30 shows the ratio between the hot-wire and driver-tube temperatures, plotted against time, for runs at 100 psia stagnation pressure. These initial measurements were made once at each tunnel location. The temperature in the nozzle appears to drop linearly with time, as the driver tube gas cools due to expansion. It is believed that the scatter between measurements at different locations is comparable to the run-to-run scatter, but repeated measurements and measurements at different locations are needed to confirm this.

Summary of Quiet-Flow Development Issues

Possible causes of the early transition on the nozzle wall include:

1. Fluctuations generated at the nozzle throat due to problems with the bleed-slot flow. Although

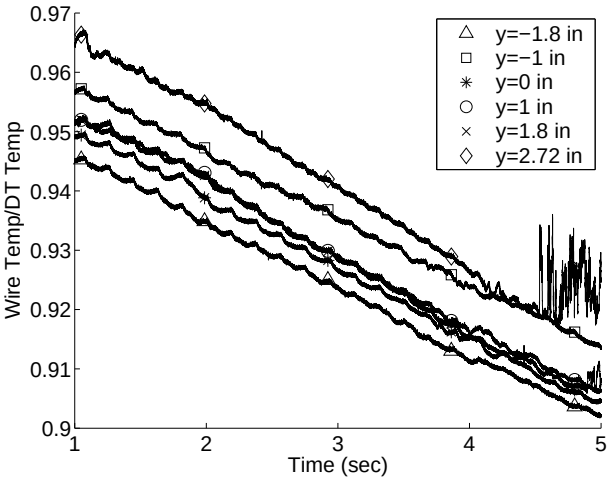

Figure 30: Temperature Measurements in Nozzle

several designs have produced similar results, this possibility still cannot be ruled out. Computations of the bleed-slot flow are to be carried out by Doyle Knight's group at Rutgers, to aid in assessing this uncertainty.

2. A nozzle-wall temperature distribution that decreases much more rapidly downstream than was initially expected. However, computations suggest this effect should be minor, and there is no evidence to suggest it could cause transition in the way observed.

3. A 0.001-0.002-inch ($Re_k < 12$) rearward-facing step at the downstream end of the electroform [28]. Here, Re_k is a roughness Reynolds number based on the height of the peak roughness, and the conditions in a smooth-wall boundary layer at the roughness height. However, this step was dramatically reduced by the fall 2002 polishing, without noticeable effect [14].

4. Insufficient polish on the downstream nozzle sections (although $Re_k < 12$). However, the fall 2002 polish had no noticeable effect.

5. Fluctuations or nonuniformity in the driver tube flow that lead to early transition. The preliminary measurements shown above are only beginning to address this issue; the results so far leave much uncertainty.

6. Some fundamental problem with the use of a very long nozzle which is not captured by the e^N analysis. This seems unlikely, since transition seems to flash forward along the whole downstream half of the nozzle at about the same pressure.

7. Noise propagated upstream from the diffuser section. Measurements reported in Ref. [15] show that the original diffuser centerbody caused separation in the nozzle-wall boundary layer when it began to drop laminar. Measurements in the Langley Mach-6 quiet nozzle showed that transition flashed forward on a flared cone when the nozzle exit shock impinged on the aft end of the cone. Upstream propagation of disturbances remained a concern, even with the new model support design, due to the jets of air from the bleed-slot suction that enter the diffuser downstream. However, when jets were removed by plumbing this bleed air directly to the vacuum tank, there was no marked effect.

8. Flaws in the throat-region polish. A small bump was felt on the bleed lip during the last assembly in late fall 2002, and it is possible that this bump is tripping transition.

9. Leaks in the low-pressure sections that cause jets of air into the nozzle, tripping the boundary layer. Although testing with soap films under pressure have not shown such leaks, small leaks may still be present. More sensitive leak tests with a helium sniffer are to be carried out.

10. Vibrations of the bleed lip, introducing disturbances that trip the flow. The tunnel vibrates when the flow starts up, but although these vibrations can clearly be felt, they seem to damp within a second or two. However, the onset of transition seems to occur at the same pressure, regardless of whether this pressure is at the beginning or the end of a run, making this cause seem less likely. The Mach-4 tunnel did not have this problem, but it did not use throat suction either, and the bleed lips may be more sensitive to vibration, particularly in the transverse direction.

Summary

Purdue University continues to develop the 9.5-inch Mach-6 Boeing/AFOSR Mach-6 Quiet Tunnel. The tunnel is being modified to run at higher pressures, with presumably conventional noise, to study transition and the transition mechanisms for blunt cones at angle of attack. Hot-wire measurements on sharp

cones show disturbances that may be related to instabilities, and preliminary calibrations have been obtained.

The main focus of the work remains the search for high Reynolds number quiet flow. Additional measurements confirm that the flow in the downstream half of the nozzle drops quiet at about 8 psia at all measured stations, suggesting a bypass of the usual linear instabilities. The very long nozzle design does not appear to be a factor in the early transition.

Downstream disturbances propagating upstream through the boundary layer have been a concern. The bleed-slot air that previously reentered the diffuser in the form of jets was plumbed directly to the vacuum tank, eliminating a major source of downstream disturbances. However, this had no effect on the onset of quiet flow at about 8 psia. Earlier measurements of the static pressure fluctuations in the diffuser associated high fluctuation levels with laminar nozzle-wall boundary layers. However, additional measurements suggest that these high diffuser fluctuation levels only occur near the onset of quiet flow, and not at higher pressures. It now seems less likely that the diffuser fluctuations are tripping the upstream flow.

An apparatus was developed and used to make initial hot-wire measurements of the fluctuations in the contraction entrance. While the RMS voltage fluctuations are two orders of magnitude below the mean, they are an order of magnitude above the prerun noise. There is also some evidence of nonuniformities in the mean flow. However, these measurements were obtained with poor control of the driver temperatures. Calibrated and repeated measurements are needed to assess this source of disturbances.

Finally, progress was made with the facility and instrumentation. A new sting support was installed, with greatly improved streamlining that eliminates upstream nozzle-wall boundary layer separation. A new boost pump is being installed for high Reynolds number operation, and preliminary condensation measurements indicate that a limited amount of supercooling may be feasible. Hot wire calibration efforts also continue, along with measurements of instabilities in the boundary layer on sharp cones under conventional noise, which have not yet yielded clear results.

Acknowledgements

The research is funded by AFOSR under grant F49620-03-1-0030, by Sandia National Laboratory under contract 80377, and by NASA Langley, under grant NAG-1-02047. Additional support was provided by Northrop-Grumman. Scott Berry contributed to this paper while visiting on a Thompson Fellowship from NASA Langley. Frank Chen and Steve Wilkinson from NASA Langley continued to provide occasional assistance in making the best possible use of information available from the earlier NASA Langley quiet-tunnel development effort.

REFERENCES

[1] Scott A. Berry, Thomas J. Horvath, Brian R. Hollis, Richard A. Thompson, and H. Harris Hamilton II. X-33 hypersonic boundary layer transition. Paper 99-3560, AIAA, June 1999.

[2] H.A. Korejwo and M.S. Holden. Ground test facilities for aerothermal and aero-optical evaluation of hypersonic interceptors. Paper 92-1074, AIAA, February 1992.

[3] AGARD, editor. *Sustained Hypersonic Flight*. AGARD, April 1997. CP-600, vol. 3.

[4] Tony C. Lin, Wallis R. Grabowsky, and Kevin E. Yelmgren. The search for optimum configurations for re-entry vehicles. *J. of Spacecraft and Rockets*, 21(2):142–149, March-April 1984.

[5] I.E. Beckwith and C.G. Miller III. Aerothermodynamics and transition in high-speed wind tunnels at NASA Langley. *Annual Review of Fluid Mechanics*, 22:419–439, 1990.

[6] Steven P. Schneider. Effects of high-speed tunnel noise on laminar-turbulent transition. *Journal of Spacecraft and Rockets*, 38(3):323–333, May–June 2001.

[7] Steven P. Schneider. Flight data for boundary-layer transition at hypersonic and supersonic speeds. *Journal of Spacecraft and Rockets*, 36(1):8–20, 1999.

[8] S. P. Wilkinson, S. G. Anders, and F.-J. Chen. Status of Langley quiet flow facility developments. Paper 94-2498, AIAA, June 1994.

[9] I. Beckwith, T. Creel, F. Chen, and J. Kendall. Freestream noise and transition measurements on a cone in a Mach-3.5 pilot low-disturbance tunnel. Technical Paper 2180, NASA, 1983.

[10] Alan E. Blanchard, Jason T. Lachowicz, and Stephen P. Wilkinson. NASA Langley Mach 6 quiet wind-tunnel performance. *AIAA Journal*, 35(1):23–28, January 1997.

[11] S. P. Schneider and C. E. Haven. Quiet-flow Ludwieg tube for high-speed transition research. *AIAA Journal*, 33(4):688–693, April 1995.

[12] Steven P. Schneider. Design of a Mach-6 quiet-flow wind-tunnel nozzle using the e**N method for transition estimation. Paper 98-0547, AIAA, January 1998.

[13] Steven P. Schneider, Shin Matsumura, Shann Rufer, Craig Skoch, and Erick Swanson. Progress in the operation of the Boeing/AFOSR Mach-6 quiet tunnel. Paper 2002-3033, AIAA, June 2002.

[14] Steven P. Schneider, Shin Matsumura, Shann Rufer, Craig Skoch, and Erick Swanson. Hypersonic stability and transition experiments on blunt cones and a generic scramjet forebody. Paper 2003-1130, AIAA, January 2003.

[15] Steven P. Schneider, Craig Skoch, Shann Rufer, and Erick Swanson. Hypersonic transition research in the Boeing/AFOSR Mach-6 quiet tunnel. Paper 2003-3450, AIAA, June 2003.

[16] Phillip M. Schneider. Flow measurements in a Mach 4 axisymmetric jet. Purdue University, School of Aeronautics and Astronautics. A 29 page laboratory report with 11 figures, May 1999.

[17] Phillip M. Schneider. Design and construction of a Mach 6 hot wire calibration jet. Purdue University, School of Aeronautics and Astronautics. A 30 page laboratory report, plus extensive appendices, December 1998.

[18] Steven P. Schneider, Shann Rufer, Laura Randall, and Craig Skoch. Shakedown of the Purdue Mach-6 quiet-flow Ludwieg tube. Paper 2001-0457, AIAA, January 2001.

[19] Steven P. Schneider. Hypersonic laminar-turbulent transition on circular cones and scramjet forebodies. *Progress in Aerospace Sciences*, 40, 2004. To appear.

[20] K.F. Stetson. Nosetip bluntness effects on cone frustum boundary layer transition in hypersonic flow. Paper 83-1763, AIAA, July 1983.

[21] J. F. Muir and A. A. Trujillo. Experimental investigation of the effects of nose bluntness, freestream Reynolds number, and angle of attack on cone boundary layer transition at a Mach number of 6. Paper 72-216, AIAA, January 1972.

[22] F.G. Keyes. A summary of viscosity and heat-conduction data for He, A, H_2, O_2, CO, CO_2, H_2O, and air. *Transactions of the ASME*, 73:589–596, 1951.

[23] P.P. Wegener and L.M. Mack. Condensation in supersonic and hypersonic wind tunnels. *Advances in Applied Mechanics*, 5:307–447, 1958.

[24] Dan E. Marren and John F. Lafferty. Experimental determination of the limits of supercooling in the NSWC hypervelocity wind tunnel no. 9. Paper 94-0199, AIAA, January 1994.

[25] Steven P. Schneider. Initial shakedown of the Purdue Mach-6 quiet-flow Ludwieg tube. Paper 2000-2592, AIAA, June 2000.

[26] Steven P. Schneider, Craig Skoch, Shann Rufer, Shin Matsumura, and Erick Swanson. Transition research in the Boeing/AFOSR Mach-6 quiet tunnel. Paper 2002-0302, AIAA, January 2002.

[27] Steven P. Schneider. Design and fabrication of a 9-inch Mach-6 quiet-flow Ludwieg tube. Paper 98-2511, AIAA, June 1998.

[28] Steven P. Schneider and Craig Skoch. Mean flow and noise measurements in the Purdue Mach-6 quiet-flow Ludwieg tube. Paper 2001-2778, AIAA, June 2001.